JOURNAL OF MATERIALS SCIENCE 27 (1992) 4858–4870

Phase-property study of semiconductor selenium

Part II *Double-phase system*

M. F. KOTKATA
Physics Department, Faculty of Science, Ain Shams University, Cairo, Egypt

An understanding of the transition from amorphous to crystalline phase is of scientific as well as technological interest, as it defines the operating limits of the materials used for technical applications. For the case of amorphous selenium, this is related to the erasure time in optical data storage applications and to the optical recording energy in holographic applications. This review provides substantial theoretical and experimental results regarding the dependence of different properties on the geometrical structure of a double-phase selenium system. This includes, the time–temperature–transformation (TTT) diagrams for amorphous solid–crystal, and amorphous liquid–crystal mixture phases together with different kinetic and thermodynamic aspects for both isothermal and scanning thermal conditions.

1. Introduction

The heating or cooling of a material from its amorphous solid or amorphous liquid states, respectively, causes continuous changes in its local structure as well as its degree of crystallinity. Kinetic studies of such changes can be carried out using non-isothermal (continuous heating) or isothermal experimental analysis of a physical property. This represents an average or effective property of a double-phase system. The term "double-phase" is derived from the fact that at any moment during the transitional change, there is a combination of the random (amorphous solid or amorphous liquid) and the crystalline modifications, or phases, of the material. In attempting a property–content characterization, two aspects must be considered: the dependence of the property on the volume fraction of each of the constituent phases and on their relative distribution in the matrix. The relative distribution of phases has a great effect on some properties such as electrical and thermal conductivities, despite not having any influence on other properties such as density, specific volume or dielectric permittivity. However, this kind of dependence on the geometrical structure becomes more pronounced if the properties of the constituent phases are markedly different. In the case of semiconductor selenium, the electrical conductivities, σ_a (conductivity of the amorphous phase), and σ_c (conductivity of the crystalline phase), vary appreciably, i.e. by four to six orders of magnitude [1].

Amorphous selenium (a-Se) has a strong tendency to crystallize. Several factors have been shown to promote crystallization of a-Se, such as elevated temperature [2–5], light [6, 7], electric field and current [6, 8], ultrasonic vibrations [8], and electron and ion bombardment [9–11]. In this paper, some physical and thermodynamical studies have been performed to characterize a double-phase selenium system where a number of our previously obtained results are considered. Regarding the isothermal processes, kinetic studies have been done by considering different effective properties of a double-phase system (amorphous with crystalline or supercooled liquid with crystalline) to define the volume fraction of each constituent phase and its variation with time in terms of several formulations connecting the individual properties of the two constituent phases. For scanning (non-isothermal) processes, the variation of the transformed weight fraction with temperature has been defined and kinetic data have been conducted.

2. Glass-formation tendency

A useful glass-formation parameter, known as K_{gl}, has been deduced by Hruby [12]

$$K_{gl} = (T_{c1} - T_g)/(T_m - T_{cl}) \quad (1)$$

where the assumptions considered in its derivation are reviewed in [12, 13]. This parameter can be determined from differential thermal analysis (DTA) of a glassy sample. It is demonstrated to be a valid indicator of glass-formation tendency, for a wide range of materials, with good glass formers having values of $K_{gl} \geqslant 0.1$ [13, 14].

As mentioned by Thornburg [13], the parameter K_{gl} involves a kinetic parameter, T_{c1}, a second-order transformation parameter, T_g, and a first-order transformation parameter, T_m. For samples quenched under the same conditions, i.e. having the same concentration of critical nuclei at the start of the heating run, the onset of crystallization, T_{c1}, will be strongly dependent on the heating rate $\phi = dT/dt$. Because the glass transition, T_g, and melting, T_m, temperatures are not typically rate dependent, K_{gl} will depend strongly

0022–2461

on the heating rate as well. This has been demonstrated by analysing the rate dependence of thermograms taken on 25 mg powdered selenium samples. Details of the DTA and of the experimental arrangement are given in [15]. Nine DTA scans at different rates in the range 0.5–100 °C min^{-1} have been carried out for selenium samples prepared under vacuum (10^{-6} torr; 1 torr = 133.322 Pa) by iced water quenching from the melts (350 °C for 3 h) of 99.999% purity pellets. Fig. 1 shows, as an example, a typical DTA dynamic scan obtained by continuous heating at a rate of 10 °C min^{-1} under a dry nitrogen atmosphere. This thermogram, like those at the other rates, is characterized by the presence of an endothermic effect of softening at $T = T_g$. Here, it is worth mentioning that T_{c1}, T_{c2} and T_{c3} correspond to the onset (dynamic crystallization temperature), midpoint (where the rate of crystallization is maximum) and completion of crystallization, respectively. Following the crystallization exotherm, an endotherm due to melting of the crystalline phase begins at a temperature $T = T_m$. The DTA in the region of T_g shows little evidence of stored strain energy in the sample scanned at the lowest rate, 0.5 °C min^{-1}. This evidence increases and becomes more pronounced with the increase in ϕ. The thermograms also indicated an increase in the sharpness of the exothermic crystallization peak with ϕ.

The time–temperature–transformation (TTT) diagram determined from the DTA scan at different rates is shown in Fig. 2. It indicates that $T_m = 220$ °C is rate independent as expected. An apparent rate dependence of T_g is observed for low (< 5 °C min^{-1}) and high (> 30 °C min^{-1}) heating rates. The value of T_{c1} increases with ϕ because less time is spent at each temperature. In fact, the three crystallization parameters T_{c1}, T_{c2} and T_{c3} are extremely rate dependent as is seen from Fig. 2. Fig. 3 shows the difference in transformation temperatures $(T_{c1} - T_g)$ and $(T_m - T_{c1})$ against ϕ for selenium samples. The rate dependence is also apparent in a plot of K_{gl} against ϕ. Over the heating rate range 0.5–100 °C min^{-1}, K_{gl}

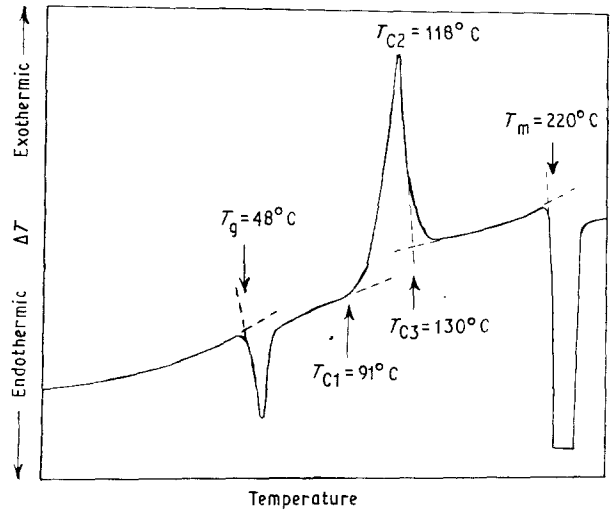

Figure 1 Typical DTA thermogram of a g-Se(350 °C) sample exhibiting a clearly defined glass transition endotherm, a crystallization exotherm, and a melting endotherm. Scan rate = 10 °C min^{-1}.

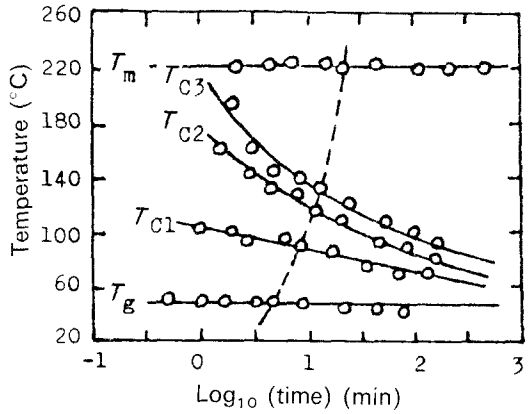

Figure 2 The time–temperature–transformation diagram for g-Se(350 °C) samples. T_g is the glass transition temperature; T_{c1}, T_{c2} and T_{c3} correspond to the onset, midpoint and end of the crystallization temperature; and T_m is the melting point.

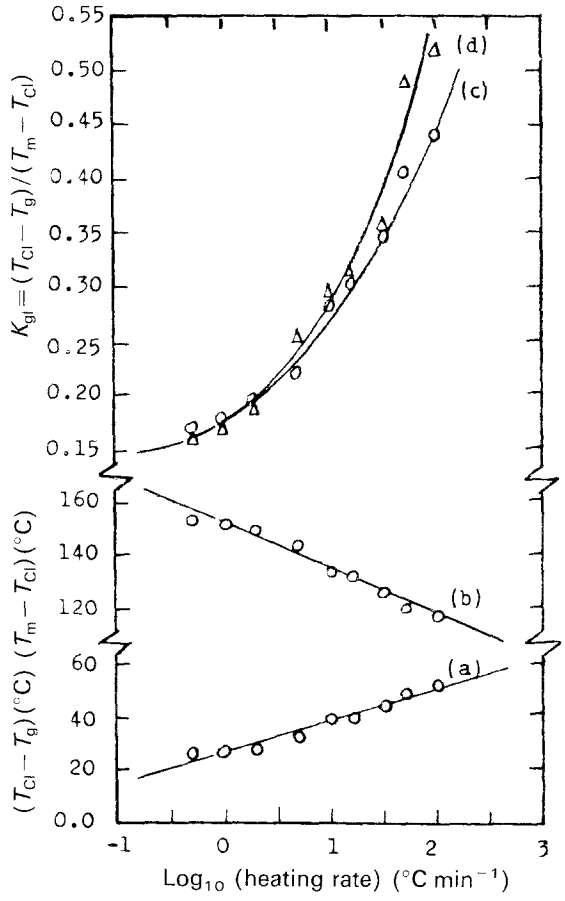

Figure 3 Difference in transformation temperatures against heating rate for g-Se(350 °C) samples.

increases by nearly a factor of 3, Fig. 3c. If T_g is taken as a constant for all heating rates ($T_g = 48$ °C), the rate dependence of K_{gl} is even more pronounced, Fig. 3d. The structural relaxation processes occurring in the glass transition region have been recently examined by DSC measurements [16].

Fig. 4 shows the heating rate dependence of T_{c2} for two sets of powder selenium samples, labelled g-Se (350 °C) and g-Se (1000 °C) according to their temperature of synthesis, T_s, before quenching. The figure indicates that the value of T_{c2} increases with an increase in ϕ or an increase in T_s. The increase in T_{c2},

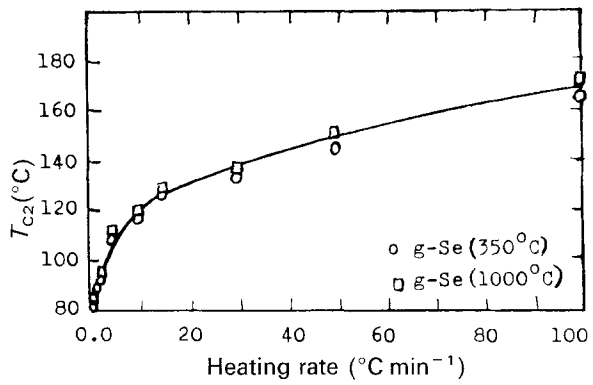

Figure 4 The heating rate dependence of the temperature T_{c2} at which the crystallization rate is maximum for two sets of selenium samples: (○) g-Se(350 °C), (□) g-Se(1000° C).

due to T_s, changes from 1 °C to 7 °C in the range 0.5–100 °C min^{-1} and it is more pronounced at higher ϕ. The change of T_{c2} with ϕ leads to the calculation of the activation energy of crystallization as will be shown in Section 6.

3. Fractional volume of a double-phase system

The density, X-ray diffraction, and direct current (d.c.) conductivity were measured for a series of double-phase selenium samples. The samples were prepared by pressing mixed powders depending on the fractional volume of both glassy and crystalline phases [17].

The effect of the fractional volumes in the double-phase selenium system on the hydrostatic density of samples compressed at 3×10^3 kg cm^{-2} is shown in Fig. 5. The figure indicates that the increase in the crystalline part from 0.0%–100% leads to a monotonic increase in the measured density from 4.07 g cm^{-3} to 4.63 g cm^{-3}. A deviation from these values might occur only if the measurements are carried out on mixed powder samples compressed at other pressures. The figure also shows the theoretical values of the density calculated using the density of bulk glassy (4.28 g cm^{-3}) and bulk crystalline (4.75 g cm^{-3}) selenium samples.

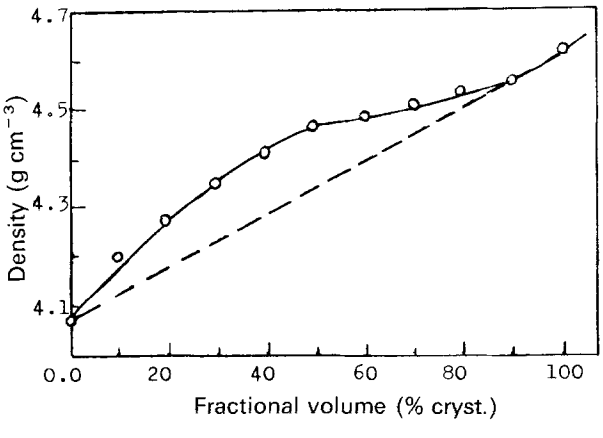

Figure 5 Fractional volume dependence of density for double-phase compressed powder selenium samples. (—○—) Experimental, (– – –) theoretical.

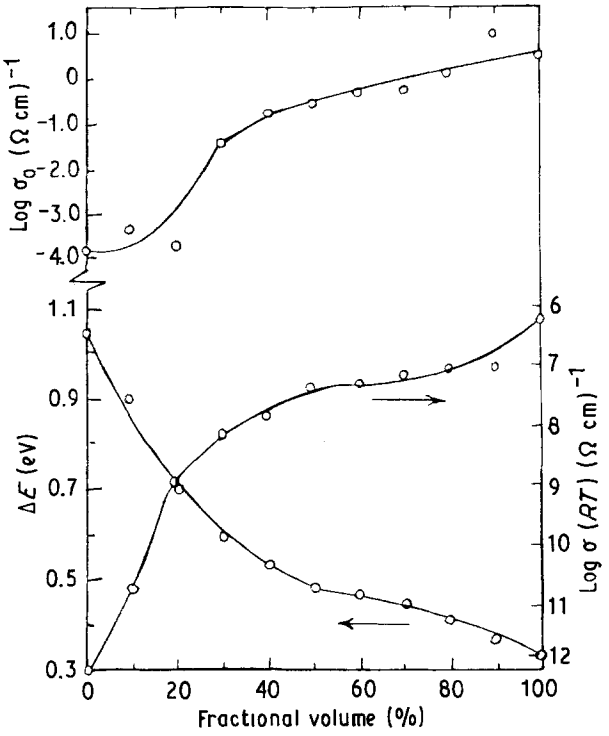

Figure 6 Fractional volume dependence of electrical characteristic quantities, ΔE, $\sigma(RT)$ and σ_0 for double-phase compressed powder selenium samples.

Fig. 6 shows the fractional volume dependence of the electrical characteristic quantities: ΔE, activation energy of conduction; σ(RT), room temperature conductivity; σ_0, pre-exponential factor of the thermally activated formula: $\sigma = \sigma_0 \exp(-\Delta E/kT)$. Details of the experimental arrangement are given in [17]. The value of σ(RT) shows a gradual increase from 5.5×10^{-13} (Ω cm)$^{-1}$ to 5.25×10^{-7} (Ω cm)$^{-1}$ with the crystalline proportion of the double-phase selenium mixture samples increasing from 10% to 100%. Also, the increase in the crystalline part in the same percentage range leads to a gradual decrease in ΔE from 0.9 eV to 0.34 eV. The value of σ_0 varies between 5×10^{-4} and 2.75 (Ω cm)$^{-1}$. These values of σ_0 lie in the range of 10^{-5}–10^8 (Ω cm)$^{-1}$ that is reported to fit most of the experimental data for other systems, both amorphous and crystalline [18]. Fig. 7 indicates a linear dependence between the pre-exponential factor, σ_0, and its activation energy, ΔE.

4. Thermal cyclic scanning

Fig. 8 shows a typical example of DTA scanning taken on 25 mg powdered g-Se (800 °C) at a constant rate of 15 °C min^{-1} during three consecutive heating–cooling cycles. On Run a, during the first heating cycle, the thermogram exhibits a glass transition, T_g, at 48 °C, an exothermic peak corresponds to the transition region (amorphous-to-crystal) with a maximum crystallization rate occurring at $T_{c2} = 115$ °C, and an endothermic peak results from the melting of the crystalline material at $T_m = 220$ °C.

In contrast to the sharply defined exothermic peak displayed during sample heating, a broadened peak,

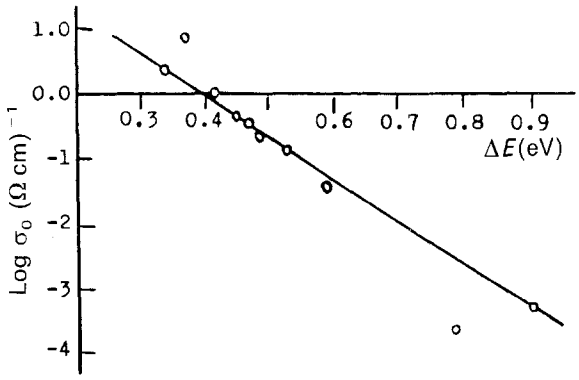

Figure 7 The pre-exponential factor, σ_0, of the electrical conductivity as a function of its activation energy, ΔE, for double-phase selenium samples.

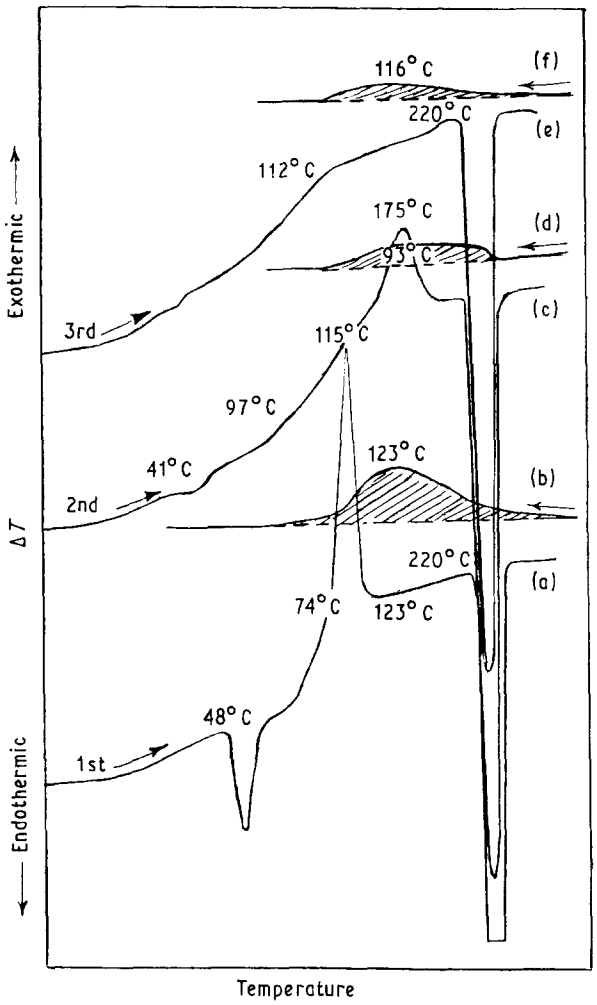

Figure 8 DTA scanning of g-Se(350 °C) during three consecutive heating-cooling cycles at 15 °C min^{-1}.

observed on Run b, during sample cooling, corresponds to a transition region (supercooled liquid-to-crystal) with a maximum peak at $T_1 = 123$ °C. The beginning of the supercooled exothermic peak starts approximately at the end of the heating endothermic peak and shifts towards the lower temperature scale. Such an observation of hysteresis suggests that the transformations should not occur at the point where the free energies are exactly equal. More often than not, such a situation could arise because of kinetic reasons. This has been supported by the results obtained when heating a sample at a relatively high rate (≈ 30 °C min^{-1}) and cooling it at a much lower rate (≈ 2 °C min^{-1}). Factors such as particle size, methods of preparation, thermal history, and heating–cooling scheme appear to affect the magnitude of thermal hysteresis. The second heating, Run c, produces a glass transition step at 41 °C, a crystallization peak with a maximum rate at 175 °C, and a melting point at 220 °C, as in Run a, with some differences in detail. This is probably associated with the form of the material at the beginning of the temperature rise. Before the first heating, Run a, the material was in a powder form, while before the second heating, Run c, the material was in a glassy solid (melted-down) form, having been melted in Run a. Here, it is worth mentioning that crystals grow more readily from powdered glass than from a massive (large solid pieces) one, i.e. it seems that nucleation is easier in the powdered material. It is assumed that less of the material is crystallized (and then melted) in the second heating than in the first heating; also it appears consistent with this suggestion about powdering that the crystallization peak in Run c begins only at a higher temperature than that in Run a (97 and 74 °C, respectively). The second and third cooling cycles, Runs d and f, resembled Run b but with smaller size of the supercooled exothermic crystallization peak. This reflects the smallest exothermic peak viewed in crystallization during the third heating cycle, Run e.

5. Thermal spectrum of d.c. conductivity

The change in d.c. conductivity, σ, of g-Se during a consecutive heating–cooling cycle within the temperature range $T_g > T > T_m$ is shown in Fig. 9. The technique applied for measuring $\sigma = f(T)$ is that used previously [19–21]. As mentioned earlier by Kauzmann [22], the experimental glass transition is thermodynamically irreversible. The glass transition almost depends upon the time-scale of the experimental measurement, e.g. of the heat capacity, C_p, relative to the relaxation times of the particular degrees of freedom which are excited [23].

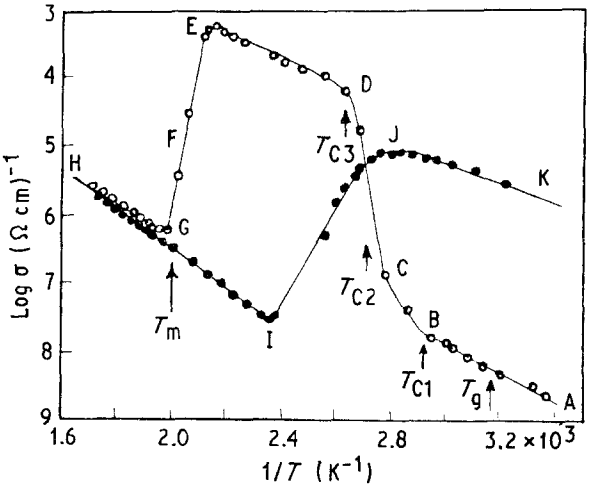

Figure 9 (a) Thermal spectrum of the electrical conductivity, and (b) DTA data of g-Se(350 °C) at 15° C min^{-1}.

Looking at the conduction spectrum of Fig. 9, one can estimate that a deviation from linearity (where there is only one Se-phase; AB, amorphous; GH, liquid; and JK, crystal) on the $\log\sigma = f(1/T, \mathrm{K})$ curves occurred at the beginning or during the peak position of the DTA heating scan (Figs 1 and 8). Point B (70 °C) represents the beginning of the amorphous-to-crystalline transformation. Close to this transition temperature, a deviation from the linearity of $\log\sigma = f(1/T)$ starts where the maximum crystallization speed is attained near Point C (93 °C). The melting temperature lies between Points E and G (220 °C). Upon cooling a liquid below its melting point, it will either crystallize or form a glass. During crystallization the viscosity, energy, volume, internal energy and hence σ change discontinuously, and the transformation is first order. In glass formation, however, these properties change continuously, although the change is relatively rapid in the vicinity of the glass transition. In Fig. 9, Point I (148 °C) represents the beginning of the liquid-to-crystalline transition during the cooling cycle.

Before and after the anomalies, the function $\log\sigma = f(1/T)$ could be well represented by straight sections verifying the Arrhenius thermal activation formula previously mentioned. The electrical characteristic values of the conduction process for the three single phases of selenium are given and discussed in Part I [1].

6. Kinetics of continuously thermally induced transformation

Crystallization of amorphous solids is a phase transformation of the type: solid phase 1 (amorphous) → solid phase 2 (crystal), and is known to proceed by nucleation and growth mechanisms, both of which are governed by separate activation energies [24, 25]. In the literature, several methods have been developed for the use of thermal analysis (DTA or DSC) in the study of non-isothermal phase transformations (cf. [26–28]). In these methods, efforts have been made to generalize the phenomenological Avrami equation [29–31], which is used in describing the kinetics of isothermally induced transformation, to the non-isothermal (or continuous) heating crystallization case. This has been done by applying simplified assumptions to determine the volume of the fraction transformed, α, (i.e. the ratio of the volume of the new phase to the total volume) from the experimental DTA (or DSC) curves and, consequently, the kinetics of the transformation process.

According to the Avrami model [29–31], the fraction, α, of material crystallized after a time, t, is given by

$$\alpha = 1 - \exp(-Kt^n) \qquad (2)$$

where the exponent n is a constant (which does not need to be an integer) depending on the details of the nucleation and growth mechanisms, and K is a temperature-dependent constant related to the rates of nucleation and growth.

The activation energy, E, of crystallization can be calculated from the DTA exotherms using a multi-scan or single-scan technique. Henderson [26], Yinnon and Uhlmann [27], and Wolny *et al.* [28], reviewed different models and techniques together with some applications to oxide and metallic glasses. An iteration and application for chalcogenide semiconductor glasses have been done by Kotkata *et al.* [14, 15, 32–37]. Applying a multi-scan technique, and for the sake of comparison, Fig. 10 shows the Kissinger (Equation 3, [38]) and Marseglia (Equation 4 [39]) continuous heating process plots for selenium. Both depend on the shifts in the T_{c2} values of the DTA thermograms with ϕ

$$\mathrm{d}[\ln(\phi/T_{c2}^2)]/\mathrm{d}(1/T_{c2}) = -E_a/R \qquad (3)$$

$$\mathrm{d}[\ln(\phi/T_{c2})]/\mathrm{d}(1/T_{c2}) = -E_a/R \qquad (4)$$

where R is the gas constant, and $E_a = E/n$ defined as the effective activation energy of crystallization. The respective values of E_a corresponding to these two models (Kissinger and Marseglia) were calculated to be 1.0 and 1.1 eV. Here, it is worth noting that each value of E_a represents an average value of the DTA results for two sets of selenium samples, g-Se(350 °C) and g-Se(1000 °C). In deriving these two models of multi-scan, it was assumed that the reaction mode n remains constant throughout the reaction (transformation) process, which is not necessarily true in all cases.

In order to determine more accurately the values of E and n for a continuously thermally induced crystallization process, a simple DTA model using a single-scan technique can be applied. The details of this model and its applicability are given in a previous publication [32], where an assumption is made that the extent of crystallization, α, is proportional to the relevant area under the DTA heating exothermic peak. The calculations lead to the respective values of 1.8 eV and 1.5 for E and n. These latter values indicate that the value of E_a is 1.2 eV, comparable to those estimated from Kissinger and Marseglia (1.0 and 1.1 eV) methods. Also, the calculations which made use of the single-scan technique [14], lead to the value

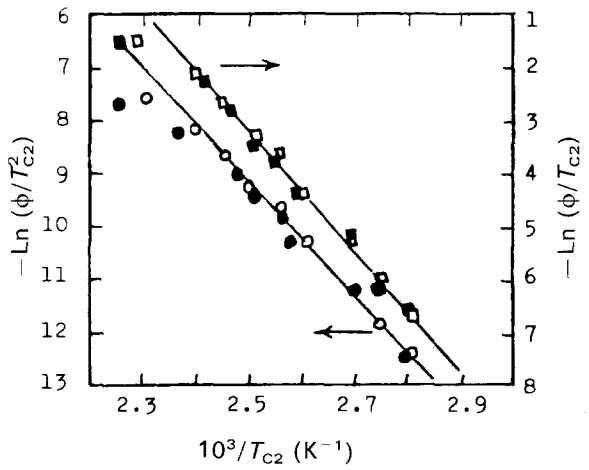

Figure 10 Determination of the crystallization activation energy from the shift of the exothermic DTA peak with the scan rate according to (○, ●) Equation 3 and (□, ■) Equation 4. Open and closed symbols indicates g-Se(350 °C) and g-Se (1000 °C), respectively.

of 10^{-2} for the reaction rate, K. Early measurements on vitreous selenium [40, 41], showed that the rate of nucleation traverses a maximum at approximately 90 °C, irrespective of the exact agreement between the results. The disagreement was attributed to the effect of the metal structure and the physical condition of the interface on the formation of nuclei. From the measurements of the velocity of crystal growth, a value of 1.05 eV has been calculated for the activation energy of the formation of hexagonal crystals from the vitreous modification of selenium [42].

The relative constancy of the obtained values of E and n for selenium during a continuous heating process seem to be due to the nucleation saturation in this process [24]. Also, n is not a purely one-dimensional process for the non-isothermal crystallization like that of the isothermal one, as we will see later in Section 10.1.

7. Morphological changes under annealing effect

The proper heat treatment of an amorphous alloy leads, generally, to the production of materials having different ratios of crystalline and amorphous fractions. In addition, it has been generally accepted, since being reported by Tammann [43], that the amorphous–crystal transformation of a material takes place through two different temperature-dependent processes: nucleation of fine crystalline centres and growth of these nuclei. The crystallization rate is supressed by reducing either one or both of these processes [44]. That is, the overall rate of transformation depends mainly on both stages which may take place at the same time. Garner [45], has reported that the number of embryos formed per unit volume relies on the temperature, impurity content and also on the thermal history of the sample. The rate of crystal growth, on the other hand, which is a function of temperature, must depend on the viscocity, diffusion, and self diffusion. The growth process has been correlated by Crystal [46, 47] with the motion of broken bonds; hole formation and hole motion. Of course, illumination plays another role in controlling the crystallization process [6, 7].

In fact, there have been many interesting similarities between selenium crystallization and crystallization of classical organic high polymers. Normally, selenium crystallization proceeds via the formation of spherulites having a lamellar structure with the width of the lamellae much less than the length of the extended selenium chain [48, 49]. This accomodation of the selenium chain is affected by the repeated folding of the chains, giving rise to the spherulites having a series of concentric rings.

A spherulite is a spherically symmetrical formation made of radial rays diverging from the centre. The simplest structural elements in a spherulite, like spherulites themselves, are interconnected by a large number of interstructural bonds in the form of the macromolecules, bundles of macromolecular or crystallized lamellar formations made mainly of chains in an extended conformation. Such bonds are formed if several macromolecules begin to crystallize simultaneously from both ends in various crystallites which are in the same spherulite or even in different spherulites. This is possible owing to a very weak correlation of the motion of the chain segments which are very far away. Such interstructural bonds combine both separate crystallites inside the lamellae.

The changes in the morphological nature of a-Se under isothermal annealing have been recorded by reflection optical microscopy (Olympus BHSM-363U), using a Nomarski differential interference system. Fig. 11 shows different stages of crystallization of a-Se isothermally annealed at 100 °C. The observed morphologies are matched with the foregoing explanation of the crystallization process of a-Se. That is, the crystallization process starts at small centres (Fig. 11a) randomly distributed in the amorphous medium. These centres gradually increase in size (Fig. 11b and c) by increasing the crystallization time. After a certain time, depending on T_a, the growth process is almost complete and the crystallites appear with boundaries in contact with each other (Fig. 11d). A progressive aligning of the spherulite branches of selenium appears with further annealing (Fig. 11e). In fact, the temperature plays another role in controlling the rate of crystal growth. Fig. 12 shows the annealing time dependence of the mean spherulite radius, $R(t)$. The latter is estimated by averaging over all the measured radii of the available spherulites in the micrograph pattern. The figure reflects the increase of $R(t)$ with both T_a and t. The effect of T_a on the texture as well as on the limiting stages of selenium crystallized for the same period have been given in our previous articles [50, 51] and confirm what we previously call "degree of perfectness of crystallinity" (DPC) evaluated using X-ray data [5].

On the other hand, Fig. 13 shows the effect of both isothermal and scanning (non-isothermal) annealing on the morphology of a-Se. Fig. 13a reflects a heterogeneous growth through the appearance of the beginning of the formation of lamellae together with some spherulite formed after an isothermal annealing for ≈ 5 h at $T_a = 70$ °C. Fig. 13b reflects a homogeneous growth resulting through the spherulites formed after a non-isothermal annealing for 34 min at a rate 5 °C min^{-1}.

8. The isothermally induced transformation

The isothermal transformation from the amorphous to the crystalline state is usually investigated by means of studying the changes of some physical parameters occurring at the structure changes. Such a parameter can be considered as a characteristic physical quantity to follow the growth of the crystallized phase in the amorphous (solid or supercooled liquid) phase.

The structural change during the amorphous–crystal (a–c) or supercooled liquid–crystal (l–c) transformations of selenium has been recorded continuously as a function of time, t, (1/2 min interval) at different isothermal annealing temperatures. At any annealing temperature, T_a, the measured parameter

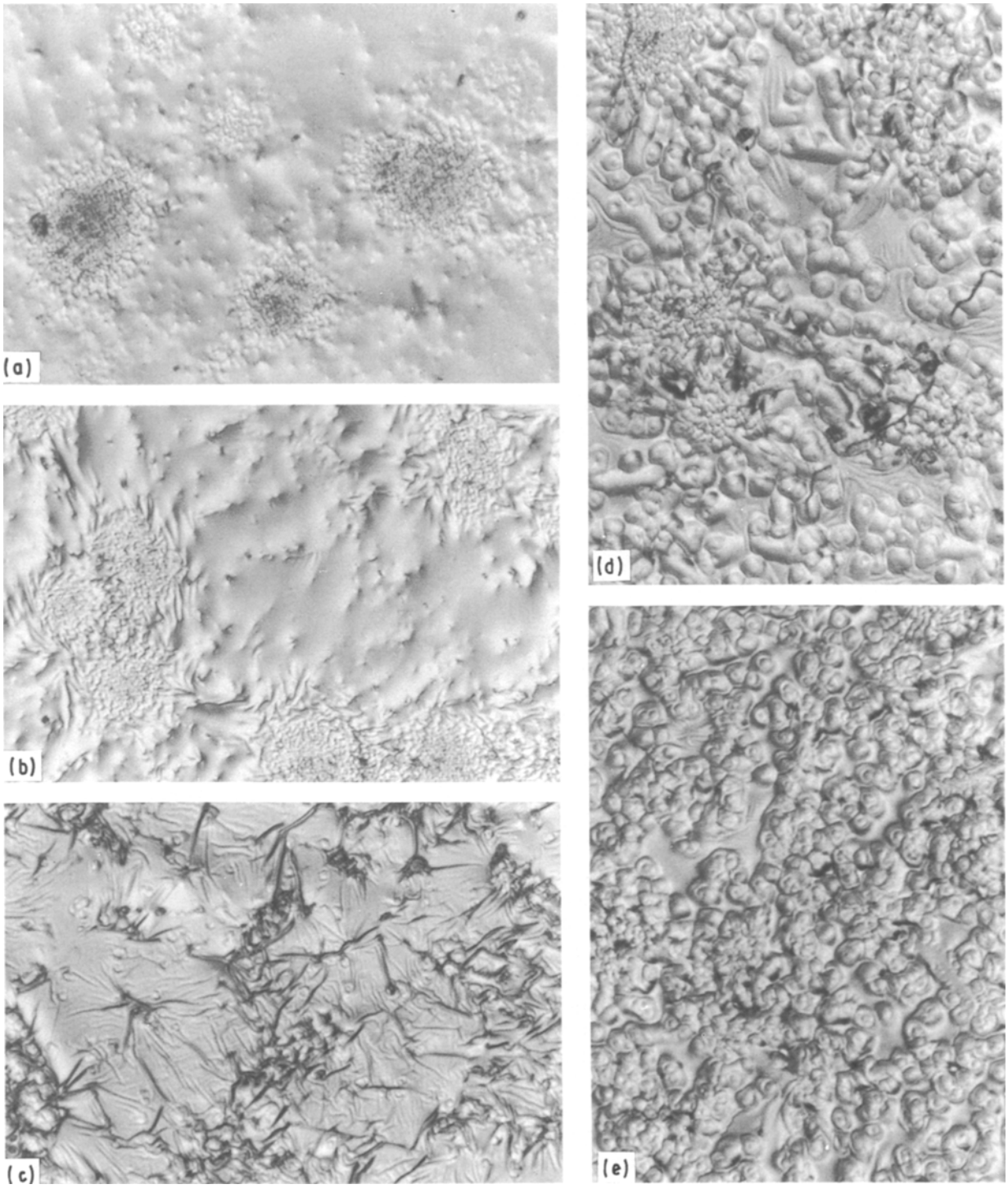

Figure 11 Optical photomicrographs illustrating different stages of crystallization of a-Se during an isothermal annealing at 100 °C.

varies with time, t, up to a certain constant limit characterizing the degree of perfectness of the material investigated. The values of T_a were selected to be in the range between the transition temperatures, T_g and T_m.

8.1. Amorphous-to-crystal phase transformation

Fig. 14 shows typical experimental plots for the time-dependence of different structural sensitive parameters for thin-film and bulk a-Se samples isothermally annealed at $T_a = 100\,°C$. The parameters considered here are: the electrical conductivity, σ, the optical transmittance, T, and the real part of the dielectric constant, ε_r. Details of the sample preparation and measuring procedures are given in previous publications [19, 21, 50–52]. Similar behaviour to that in Fig. 14 was obtained for the other annealing temperatures considered in the range 70–160 °C. Each plot for the time dependence of Fig. 14 exhibits a three-step character, namely AB, BC, and CD. As mentioned above, proper heat treatment of an amorphous material leads, in general, to the formation of a material having a mixture of crystallized and amorphous fractions. In this respect, the measured parameters σ, T, and ε_r reflect the contribution of the two mixed

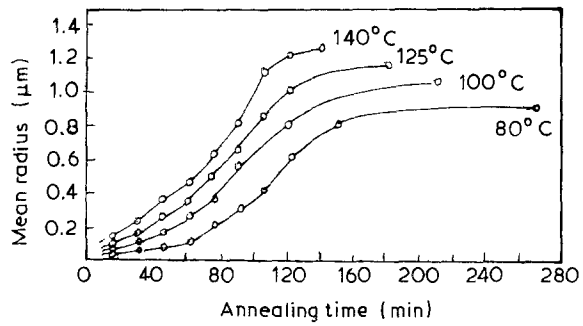

Figure 12 The annealing time dependence of the mean spherulite radius of selenium isothermally annealed at different temperatures, T_a.

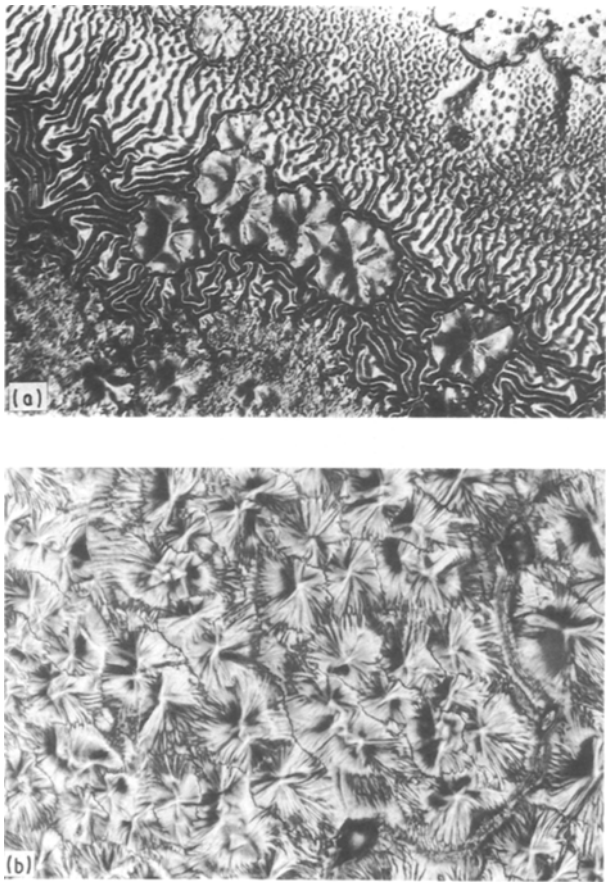

Figure 13 Optical photomicrographs of a-Se annealed under (a) isothermal and (b) non-isothermal conditions.

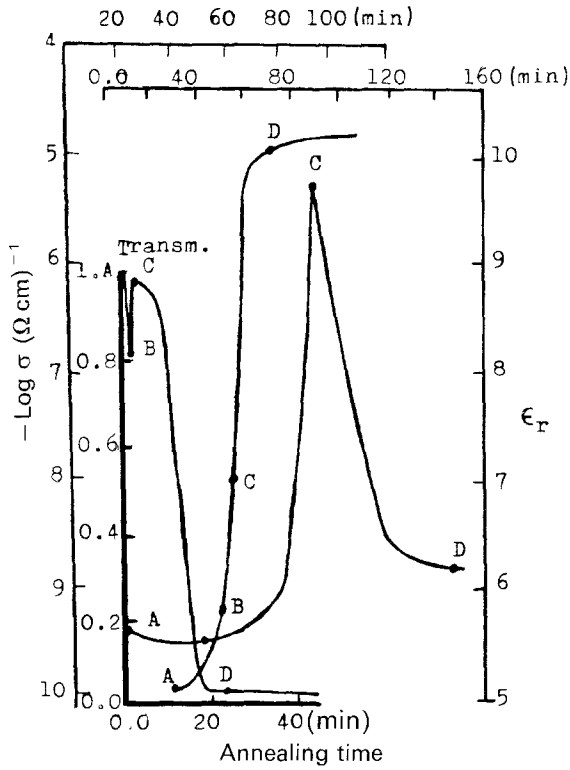

Figure 14 The annealing time dependence of d.c. conductivity, (σ), transmittance, (T), and dielectric constant, (ε_r), during the a–c transformation of a-Se at $T_a = 100\,^{\circ}C$.

phases. The slight increase in σ or decrease in ε_r during part AB (Fig. 14), results from a normal heating of the amorphous sample as transformed from room temperature to the preheated oven temperature (annealing temperature, T_a), rather than accounted for changes in geometrical or physical peculiarities. The effect of such a normal heating period appears as fast and irregular changes in T (as well as in the reflectance, R [51]) due to random scattering of the incident photons in the metastable a-Se matrix. Increasing T_a from 70 °C to 160 °C leads to a decrease in the normal heating period from about 40 min to zero. In fact, the transformation a–c passes through two distinguishable time-dependent stages: the first, BC, shows a small increase in σ, T, or ε_r relative to the pronounced change (increase in σ and ε_r, or decrease in T) during the second stage CD. The time interval BC corresponds to the formation of nuclei centres, statistically scattered through the sample volume, followed by a radial growth of independent discrete lamellae. This stage is known as primary crystallization. Such a process occurs at the same rate and in all directions. The process of primary crystallization is accompanied by a smooth liberation of heat energy associated with the transition from a non-equilibrium thermodynamic state to a rather equilibrium one and the material becomes less resistive and more transparent. In other words, one may say that the change resulting during this stage is accompanied by structural differentiation with medium-range-order and confers the properties on the low time-scale. As soon as the radial growth becomes complete, the final stage of crystallization starts (secondary crystallization); this corresponds to the part CD of the plots in Fig. 14. This last stage covers a wide range of σ, T and ε_r on the high time-scale. The change in the measured parameter is to continue until it reaches a constant limiting value (denoted by Point D) reflecting the end of the a–c transformation process. Such a value is a function of the annealing temperature and related to DPC [5]. The pronounced increase in σ results from a gradual establishment of conducting paths between electrodes through the sample. On the other hand, the marked decrease of ε_r after reaching a maximum value is mainly caused by the progressive alignment of selenium spherulite branches and the consequent decrease of the crystallite surface-to-volume ratio [6]. It should be noted that whatever the physical parameter studied, the relative time elapsed during the same transition stage (AB, BC, or CD) is approximately

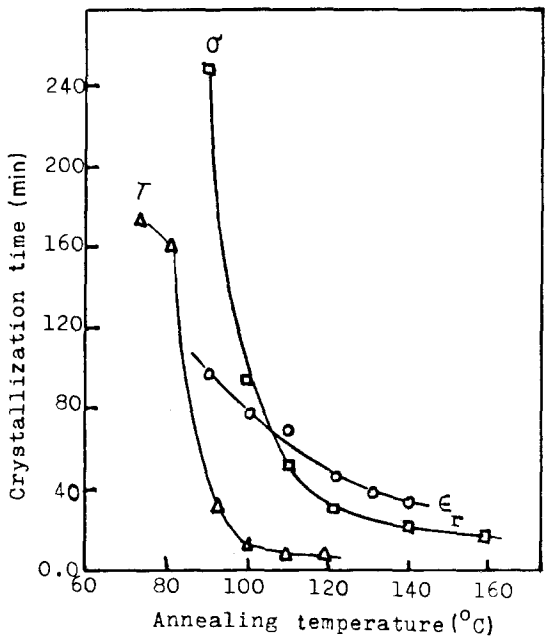

Figure 15 The annealing temperature dependence of the crystallization time, τ, as estimated from measuring the functions: σ, ε_r (bulk), T (thin film) = $f(t)$ of a-Se.

equal. Fig. 15 shows the annealing temperature dependence of the total time, τ, necessary for completing the transformation process. Increasing the value of T_a leads to the decrease of τ. The figure also indicates a shorter time, τ, in case of T (thin film) than those of σ(bulk) or ε_r(bulk).

The TTT curve obtained from the dielectric data of selenium isothermally crystallized from the amorphous solid phase is shown in Fig. 16.

8.2 Supercooled liquid-to-crystal phase transformation

Fig. 17 displays the time dependence of σ during the crystallization of selenium at two supercooling temperatures, T_{sc}, namely 80 and 130 °C. The measurement technique is given in [53]. The drop of σ at the first part AB is mainly caused by the sudden cooling of the liquid selenium as it transformed from T_s = 300 °C (> T_m) to the preheated oven temperature of super-

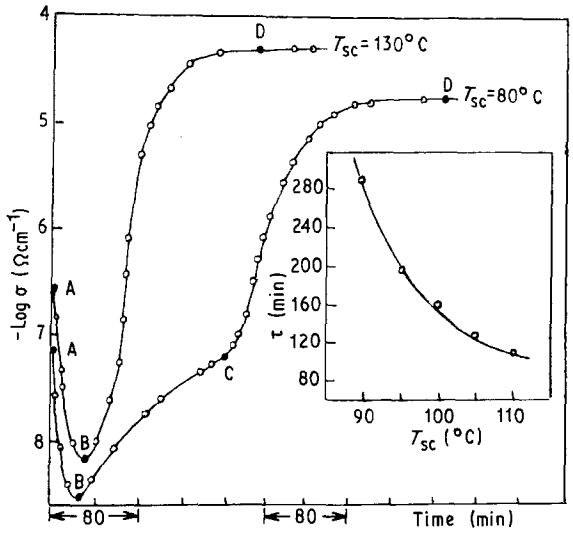

Figure 17 The annealing time dependence of d.c. conductivity, σ, during the l–c transformation of selenium at two supercooling temperatures T_{sc} = 80 and 130 ° C. The inset shows the dependence of τ on T_{sc}.

cooling, which is always maintained at a lower value than that of T_m. This decrease terminates at the moment where the sample temperature reaches that of the oven. X-ray diffraction has proved that there are no characteristic lines before Point B.

Because the crystallization from the liquid state normally proceeds by the processes of nucleation and growth, the crystallization rate is therefore supressed by reducing either one or both of these processes. For T_{sc} < 100 °C, the l–c transformation is found to occur during two stages, BC and CD. The former is related here to a structural ordering process and not to a nucleation process, as the number of nuclei is predicted to be constant, pre-determined, and does not depend on T_{sc}. This is estimated from the linearity of the plot of the function: $-\ln(1/\tau) = f[T_{sc}(T_m - T_{sc})^2]$ (Fig. 18), according to the Volmer theory [54], where $1/\tau$ is considered to be proportional to the nucleation rate and T_m is taken equal to 493 K. In such a theory, the rate of nucleation may be represented as

$$j = C_v \exp\{-C[T_{sc}(T_m - T_{sc})^2]\} \quad (5)$$

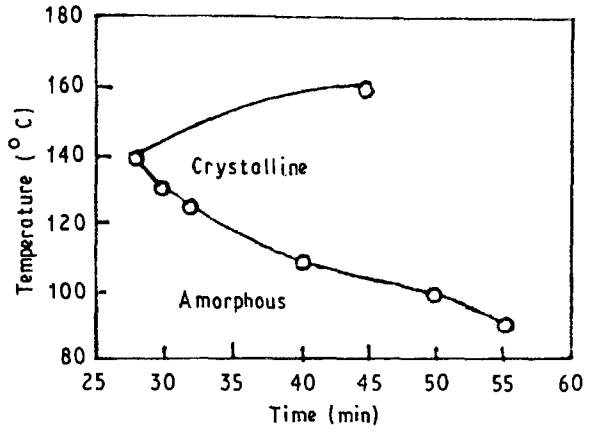

Figure 16 The time–temperature–transformation curve for selenium crystallized from the amorphous solid phase as obtained from dielectric data.

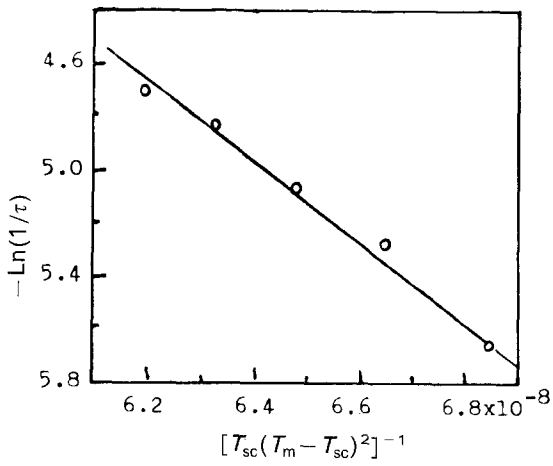

Figure 18 Relation of $-\ln(1/\tau)$ against $1/[T_{sc}(T_m - T_{sc})^2]$ for selenium.

where C_v is a constant depending on the frequency of nucleation of crystals, the velocity of their growth after nucleation, and the free energy of activation of transport. C is a parameter defining thermodynamics of the transformation. The region CD in Fig. 17 thus corresponds to the linear growth of the new phase in the supercooled liquid. For $T_{sc} > 100\,^{\circ}C$, the l–c transformation proceeds through only one smooth stage as shown in Fig. 17 for $T_{sc} = 130\,^{\circ}C$, as an example. The inset of Fig. 17 shows the T_{sc} dependence of τ, where the increase in the supercooling temperature leads to a decrease in the total time necessary to complete the transformation process.

Fig. 19 shows the TTT curves for 20%, 50%, and 80% crystallized selenium samples from the supercooled liquid phase, as calculated from d.c. conductivity data. It is believed that a more symmetrical TTT curve results from more homogeneous nucleation. The cooling rate required to avoid a given fractional crystallized volume can be estimated from the formula

$$R_c = (T_m - T_0)/t_0 \qquad (6)$$

where T_0 and t_0 are the temperature and time corresponding to the TTT knee, respectively. The value of R_c ought to decrease from $\approx 20\,^{\circ}C\,min^{-1}$ to $6\,^{\circ}C\,min^{-1}$ in order to increase the crystallized fraction from 20% to 80%.

9. Conduction models of a double-phase system

On the electrical conductivity of a mixture of amorphous and crystalline selenium, there are several formulations starting with a spatial geometrical structure of the mixed system, and the related conductivity has been derived by different authors e.g. Odelevsky [55, 56], Landauer [57], and Kirkpatrick [58]. When these models are compared with the experimental data as a function of the relative concentration of amorphous and crystalline selenium, the agreement is not even on a qualitative level [17], thus one concludes that the conjectured spatial configuration of these authors [55–58] is invalidated. This is expected for a double-phase system whose terminal conductivity values (σ_a and σ_c) differ by four to seven orders of magnitude, as in the case of selenium. The most important models [55–61] that have been used in characterizing the amorphous–crystalline mixture have been briefly reviewed [17, 62]. In this respect, Kotkata and Kandil [17] have proposed a conductivity formula where a distinctly excellent agreement with the experimental data has been obtained. The structure of this formula for a mixed system of amorphous and crystalline selenium is analysed by a derivation of the distribution function of the concentration ratios of the mixture [63]. Such a formula states

$$\sigma_m^2 = (\sigma_c/\sigma_a)^{\alpha}\,[\alpha(\sigma_c\sigma_a - \sigma_a^2) + \sigma_a^2] \qquad (7)$$

where σ_m is the conductivity of a binary matrix system, with constituents of volume fractions α and $(1 - \alpha)$ whose conductivities are σ_a and σ_c. The values of the function $\log \sigma_m = f(\alpha)$ calculated on the basis of Equation 7 are shown in Fig. 20 together with the experimental data (Fig. 6, Section 3), indicating satisfactory agreement over the whole range of α. Also, this last formula has been examined for various isothermally annealed massive selenium samples of known degree of crystallinity (as determined by X-ray analysis) and very satisfactory results are found. Here, it is worth pointing out that Equation 7 satisfies the statistical mixture condition of Odelevsky [55]; that is, when we perform the transformations $\sigma \to \sigma_a$, $\sigma_a \to \sigma_c$, $\alpha \to (1 - \alpha)$, the new σ_m is given by Equation 7.

10. Kinetics of the isothermal transformation

The generally accepted model for the crystallization kinetics under isothermal conditions is the Avrami equation (Equation 2). According to Becker [64], the energy of activation necessary for the formation of the crystalline grain, E, depends on the activation energy of the transfer of particles to the nucleus, q, and on the energy of nucleation, ΔF. The theoretical dependence of the rate constant, K, of the Avrami equation on absolute temperature, T, can be expected to exhibit an Arrhenius dependence as

$$K = K_0\exp(-\Delta F - q) = K_0\exp(-E/RT) \qquad (8)$$

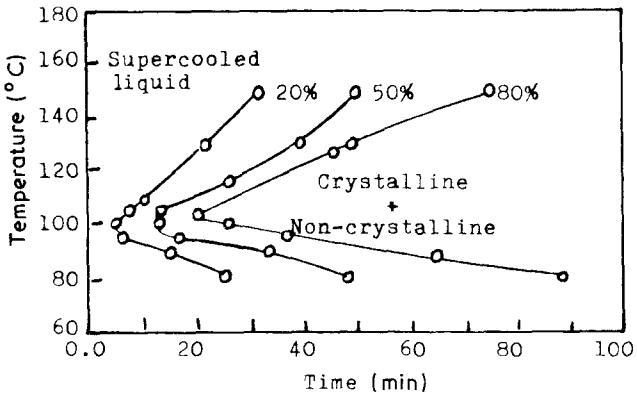

Figure 19 The time–temperature–transformation curves for 20%, 50%, and 80% crystallized selenium samples from the supercooled liquid phase obtained from d.c. conductivity data.

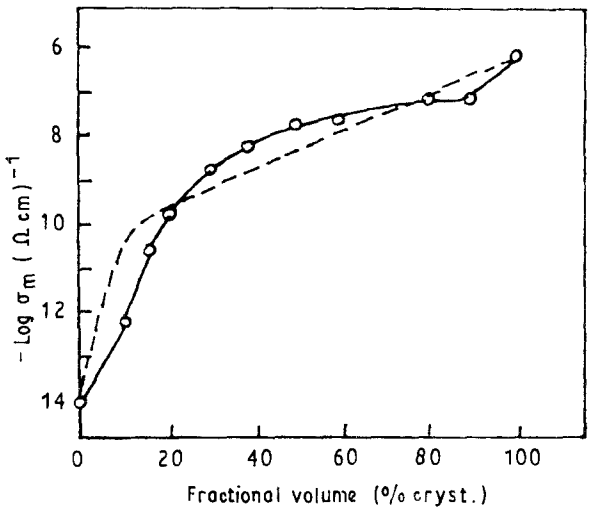

Figure 20 Fractional volume dependence of the (○) measured and (– – –) calculated conductivity, σ_m, according to Equation 7 for double-phase compressed powder selenium samples.

where K_0 is the rate constant and E is an effective activation energy for the transformation, i.e. for removal of an atom from the random (amorphous) matrix and migration across the interface on to a crystallization or diffusion to a nucleation site.

For isothermal crystallization, both E and n can be easily estimated. From Equations 1 and 8, one can write

$$\ln[-\ln(1-\alpha)] = \ln K_0 - E/RT + n\ln(t) \quad (9)$$

At constant T, a plot of $\ln[-\ln(1-\alpha)]$ against $\ln(t)$ should give a straight line of gradient defining the Avrami exponent n, and whose intercept on the ordinate at $\ln(t) = 0$ is $\ln(K)$.

10.1. The reaction mode n

The plots of α against annealing time, t, give a measure of the rate of crystal growth and also an idea about the uniformity of the crystallization process. Fig. 21 shows the time dependence of crystallinity percentage for selenium crystallized at 100 °C as calculated from different physical parameters using the following formulae

$$\alpha(t) = (\ln\sigma_m - \ln\sigma_a)/(\ln\sigma_c - \ln\sigma_a) \quad (10)$$

$$\alpha(t) = (T_m - T_a)/(T_c - T_a) \quad (11)$$

$$1/\varepsilon_m = (\alpha/\varepsilon_a) + (1-\alpha)/\varepsilon_c \quad (12)$$

where the subscripts c and a represent the values of the considered parameter (σ, T or ε_r) at the end and the initial modes, and m is that at any intermediate (growth) state of time, t. The figure indicates that the function $\alpha(\sigma, T \text{ or } \varepsilon_r) = f(t)$ is almost sigmoidal in shape, indicating an autocatalytic reaction as often observed in various kinds of solid reactions. For any of these functions, the crystallization rate curves appear to shift towards lower time scales with increasing temperature, as one might expect from the decrease in viscosity with increasing temperature of crystallization transformation, T_a. Fig. 22 shows a plot of the function $\ln[-\ln(1-\alpha) = f\ln(t)]$ for selenium during the two transformation processes (a–c and 1–c) at 100 °C. This has been done by considering the variation of the physical quantities, σ [19, 52], T [53], or ε_r[50] with time, t (Figs 14 and 17) as a structural sensitive parameter characterizing the ratio of the two constituents (amorphous solid, or supercooled liquid, with crystalline) of the double-phase system, mostly from $\alpha = 0$ to $\alpha = 1$. Similar behaviour to that of Fig. 22 has been found at the other isothermal transformation temperatures investigated.

If the assumption of spatially random nucleation and linear growth (growth rate not depending on time) are made [65], two simple cases can be distinguished for an increase in the rate of increase of nuclei: the reaction mode n can acquire increasing values up to 4 implying constant nucleation rate; n can take only

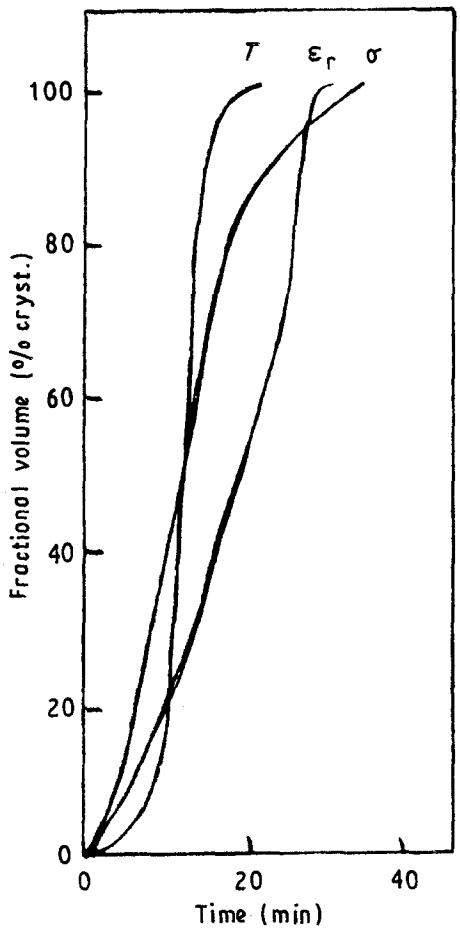

Figure 21 Crystallinity percentage plotted against annealing time for selenium crystallized at 100 °C, calculated from Equations 10–12.

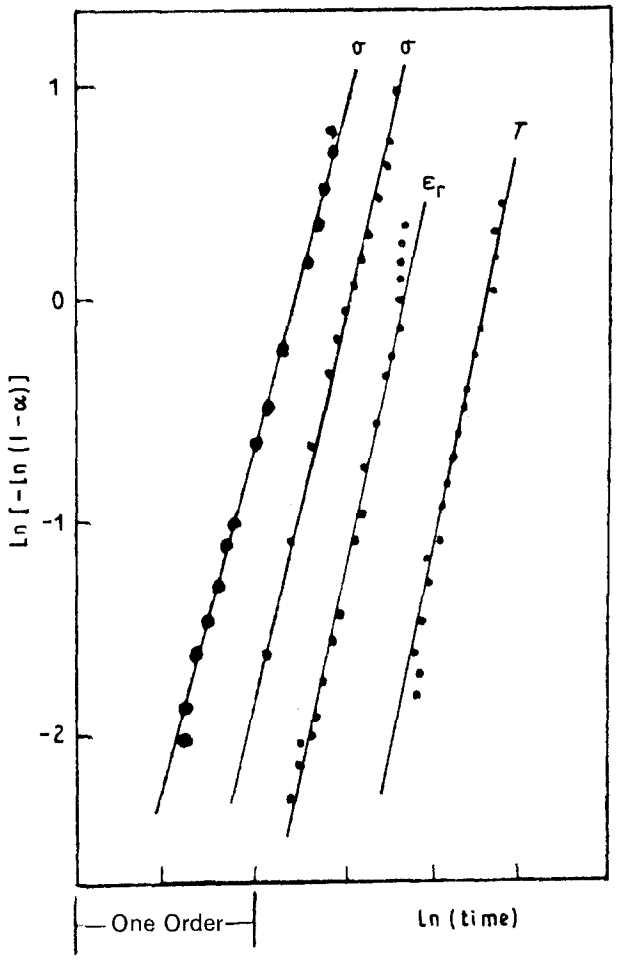

Figure 22 Kinetics of the crystallization of selenium calculated from the variation of σ, T or ε_r with time during (●) a–c and (●) 1–c at 100 °C.

three integer values, 1, 2 or 3, depending on whether it represents one, two, or three-dimensional growth implying a zero nucleation rate, i.e. growth only on pre-existing nuclei. Taking into consideration the experimental data obtained for polymer crystallization, Hay [66] has proved the possibility of half integer values of n for lateral growth or for growth controlled by diffusion. That is, $n = 5/2$ for a nucleation rate constant, and $n = 3/2$ for early site saturation of randomly placed heterogeneous nuclei.

Fig. 23 shows the variation of n with the annealing temperature for a–c and l–a isothermal transformations as calculated from the measurements of different physical parameters, together with the results of Crystal [2] calculated for a–c transformations using a densitometric method. The figure indicates that the numerical values of the different series of calculations do not agree very closely in the investigated temperature range, but all curves manifest the same trend for the temperature dependence of n. There is a decrease in the value of n in the temperature range from 70 to 100–110 °C, and then the value of n shows an increase with the annealing temperature. The low values of n lie in the range 1.3–1.6, while the high values lie in the range 2.0–2.6 for both a–c and l–c transformations using the results of σ, T, $\varepsilon_r = f(t)$. This provides evidence for different growth geometries in different temperature ranges. In fact, the high viscosity and the increased ring to chain ratio does undoubtedly control the crystallization mode of selenium on the low-temperature scale. It is to be noted that the values of n calculated by a dynamic density technique [2] agree well with our data in the low-temperature range, but do not agree at temperatures higher than 100 °C. This would give an easy explanation for the unreliability of the densitometric technique to reflect the distribution of the random and crystalline phases during the crystallization transformation of selenium, especially at high temperatures. On the other hand, the relative constancy of the values of n for both a–c and l–c processes reflects a similarity in the saturation degree of the nucleation sites, i.e. unique growth geometry. However, and according to the theory of crystallization [24], such a temperature dependence of n indicates that the process of crystallization of selenium takes place with predominance of homogeneous nucleation and one-dimensional growth, or heterogeneous nucleation and two-dimensional growth of crystallization nuclei.

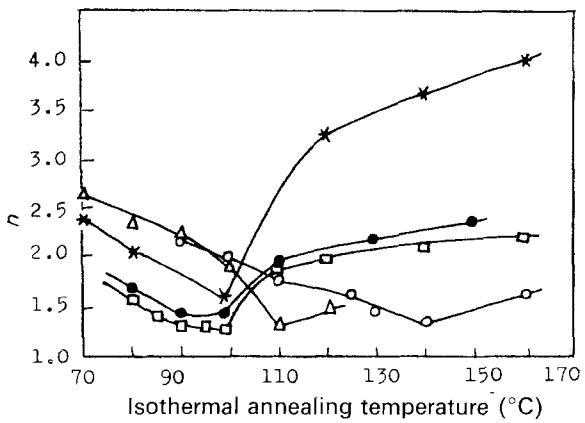

Figure 23 The annealing temperature dependence of the Avrami exponent, n, of selenium for a–c: (□) σ, (△) T and (○) ε_r; and l–c: (●) σ isothermal transformation with (*) the results obtained from densitometric data [2].

10.2. The activation energy, E

A plot of $\ln(K) = f(1/T)$ can be fitted over a certain temperature range with a straight line whose slope defines the activation energy of the process, E. For selenium during its a–c or l–c transformations, the average values of K over at least the range of $\alpha \approx 10\%–90\%$, and a least square fit to the experimental points are considered. Here, the value of E is found to be dependent on the temperature range investigated rather than on the structure-sensitive parameter considered to follow variation of the fractional volume ratio of the constituents of the double-phase selenium system. Fig. 24 shows a histogram illustrating the temperature-range dependence of E for both a–c and l–c transformations of selenium. It indicates a good agreement between the E values calculated from the different physical parameters over a certain temperature range. That is, $E = 1.2–1.3$ eV in the range 70–110 °C, and $E = 0.43–0.48$ eV for the higher temperatures up to 160 °C. In fact, a temperature dependence of E is expected. This is because the activation energy is contributed to by the activation energy of nucleation and growth, and because the activation energy of nucleation is temperature-dependent.

11. Conclusion

The objectives of this study were to control and define the ratio of the constituents of a double-phase selenium system under different conditions using various

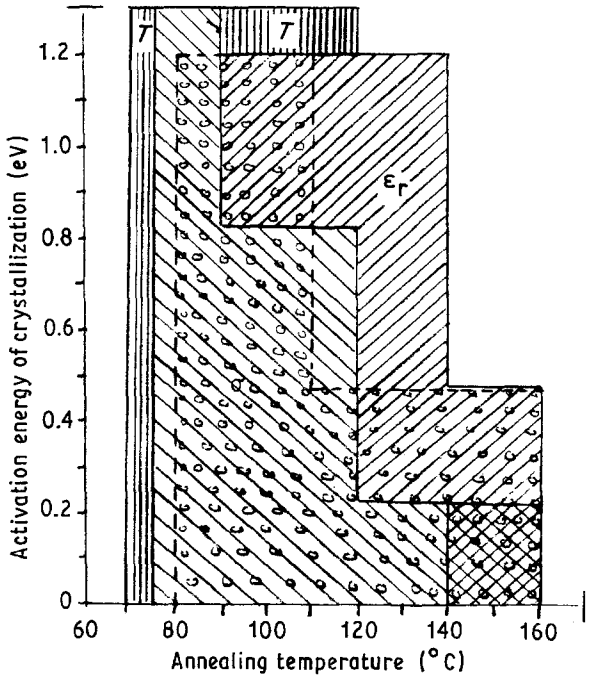

Figure 24 A histogram for the temperature-range dependence of activation energy of crystallization of selenium during (———) a–c and (– – –) l–c for data obtained from σ, T, and ε_r

techniques. This has been done through a study of the phenomena accompanying the temperature and time-induced structural changes in amorphous solid and/or supercooled liquid phases of selenium during both isothermal and scanning thermal processes. The results of direct current properties, dielectric constant and optical transmittance coupled with curves of reaction rate versus temperature for constant heating rates ($\phi = 0.5$–$100\,^{\circ}C\,min^{-1}$) have been used to demonstrate the per cent, nature and kinetics of growth phases during the transformation processes. The amorphous phase which has a high value of resistivity is characterized by a relatively low value of activation energy for transformation, and hence its crystallization can easily occur. This characteristic leads to the conclusion that the transformation of a-Se can be quickened during the erasure process for its use in optical data storage applications, as well as to decrease the optical recording energy in holographic applications.

References

1. M. F. KOTKATA, *J. Mater. Sci.* **27** (1992) 4847.
2. R. G. CRYSTAL, *J. Polym. Sci.* **8** (1970) 2153,
3. K. S. KIM and D. TURNBULL, *J. Appl. Phys.* **44** (1973) 5237.
4. W. E. BROWER and D. J. CAPO, *J. Vac. Sci. Technol.* **13** (1976) 1066.
5. M. F. KOTKATA and M. H. ALY, *Ind. J. Tech.* **22** (1984) 170.
6. J. DRESNER and G. B. STRING-FELLOW, *J. Phys. Chem. Solids* **29** (1968) 303.
7. K. S. KIM and D. TURNBULL, *J. Appl. Phys.* **45** (1974) 3447.
8. A. I. POPOV, *Phys. Chem. Glasses* **19** (1978) 43.
9. M. SHIOJIRI, *Jpn J. Appl. Phys.* **6** (1967) 163.
10. B. M. PETER, *Thin Solid Films* **26** (1975) 227.
11. H. W. PINSLER and W. E. BROWER, *J. Phys. Chem. Solids* **38** (1977) 393.
12. A. HRUBY, *Czech. J. Phys* **B22** (1972) 1187.
13. D. D. THORNBURG, *Mater. Res. Bull.* **9** (1974) 1481.
14. M. F. KOTKATA, M. H. EL-FOULY and S. A. FAYEK, *J. Mater. Sci.* **24** (1990) 2906.
15. M. F. KOTKATA, M. H. EL-FOULY, A. Z. EL-BEHAY and L. A. WAHAB, *Mater. Sci. Engng* **60** (1983) 163.
16. S. O. KASAP and S. YANNACOPOULOS, *J. Mater. Sci.* **24** (1989) 893.
17. M. F. KOTKATA and K. M. KANDIL, *Mater. Sci. Engng* **95** (1987) 287.
18. J. CORNET and D. ROSSIER, in "Proceedings of the 5th International Conference on Amorphous and Liquid Semiconductors", edited by J. Stuke and W. Brening, by Garmischparten-kirchen, 1973 (Taylor and Francis, London, 1974) p. 267.
19. M. K. EL-MOUSLY, M. F. KOTKATA and S. A. SALAM, *J. Phys. C* **11** (1978) 1077.
20. M. F. KOTKATA, *J. Non-Cryst. Solids* **59–60** (1983) 891.
21. M. F. KOTKATA and A. F. EL-DIP, *Mater. Sci. Engng* **67** (1984) 39.
22. W. KAUZMANN, *Chem. Rev.* **43** (1948) 2191.
23. L. W. WOODCOCK, in "The structure of Non-Crystalline Materials", edited by P. H. Gaskell (Taylor and Francis, London, 1977) p. 187.
24. J. W. CHRISTIAN, "Theory of Transformations in Metals and Alloys", Part I (Pergamon Press, Oxford, 1975).
25. C. N. R. RAO and K. J. RAO, "Phase Transitions in Solids" (McGraw-Hill, New York, 1978).
26. D. W. HENDERSON, *J. Non-Cryst. Solids* **30** (1979) 301.
27. H. YINNON and D. R. UHLMANN, *ibid.* **54** (1983) 253.
28. J. WOLNY, J. SOLTYS and R. KOKOSZKA, *ibid.* **91** (1987) 20
29. M. AVRAMI, *J. Chem. Phys.* **7** (1939) 1103.
30. *Idem., ibid.* **8** (1940) 212.
31. *Idem., ibid.* **9** (1941) 177.
32. M. F. KOTKATA and E. A. MAHMOUD, *Mater. Sci. Engng* **54** (1982) 163.
33. M. F. KOTKATA, M. H. EL-FOULY and M. B. EL-DEN, *Latin-Amer. J. Mettal. Mater.* **5** (1985) 28.
34. M. F. KOTKATA, M. H. EL-FOULY, S. A. FAYEK and S. A. EL-HAKIM, *Semicond. Sci. Technol.* **1** (1986) 313.
35. M. F. KOTKATA, M. H. EL-FOULY and M. A. MORSY, *J. Therm. Anal.* **32** (1987) 417.
36. M. F. KOTKATA, C. S. MOHAMED and M. M. RADWAN, *J. Mater. Sci.* **25** (1990) 482.
37. M. F. KOTKATA, M. H. EL-FOULY and S. A. FAYEK, *ibid.* **25** (1990) 2917.
38. H. E. KISSINGER, *Analyt. Chem.* **29** (1957) 1702.
39. E. A. MARSEGLIA, *J. Non-Cryst. Solids* **41** (1980) 31.
40. A. V. HIPPEL and M. C. BLOOM, *J. Chem. Phys.* **18** (1950) 1243.
41. T. SATA and H. KANEKO, *Technol. Rep. Tohoku Univ.* XIV **2** (1950) 45.
42. P. H. KECK, *J. Optic. Soc. Amer.* **42** (1952) 221.
43. G. TAMMANN, "The States of Aggregation", translated by R. F. Mehl, (Van Nostrand, New York, 1925).
44. B. G. BAGLEY, in "Amorphous and Liquid Semiconductors", edited by J. Tauc (Plenum Press, London, 1974) Ch. 1.
45. W. E. GARNER, "Chemistry of Solid State" (Butterworths, London, 1955) Ch. 6.
46. R. G. CRYSTAL, *J. Polym Sci.* **4** (1971) 187.
47. *Idem., J. Amer. Chem. (Polym. Prep).* **13** (1972) 799.
48. A. TAGER, "Physical Chemistry of Polymers", 2nd Ed (Mir, Moscow, 1978).
49. R. A. WESTBURY and W. C. COOPER, in "Selenium", edited by R. A. Zingaro and W. Cooper (Van Nostrand-Reinhold, New York, 1979).
50. M. F. KOTKATA, H. A. KHALEK, W. M. ATIA, T. PORJESZ and M. EL-SAMAHY, *J. Mater. Sci.* **20** (1985) 2973.
51. M. F. KOTKATA and F. A. EL-WAHAB, *ibid.* **25** (1990) 2379.
52. M. F. KOTKATA, G. M. KAMAL and M. K. EL-MOUSLY. *Ind. J. Tech.* **20** (1982) 390.
53. M. F. KOTKATA, A. A. EL-ELA, E. A. MAHMOUD and M. K. EL-MOUSLY, *Acta Phys. Hung.* **52** (1982) 3.
54. D. TURNBULL, *J. Chem. Phys.* **20** (1952) 411.
55. O. I. ODELEVSKY, *J. Tech. Phys. (USSR)* **21** (1951) 667.
56. *Idem., ibid.* **21** (1951) 678.
57. R. LANDAUER, *J. Appl. Phys.* **23** (1952) 779.
58. S. KIRKPATRICK, *Phys. Rev. Lett.* **27** (1971) 1722.
59. R. HOSEMANN, K. LEMM and H. KREBS, *Z. Phys. Chem. N. F.* **41** (1954) 121.
60. M. F. KOTKATA, F. M. AYAD and M. K. EL-MOUSLY, *J. Non-Cryst. Solids* **33** (1979) 13.
61. M. K. EL-MOUSLY and Z. U. BORISOVA, *Bull. Acad. Sci. (USSR) Inorg. Mater.* **3** (1967) 923.
62. M. F. KOTKATA, A. F. EL-DIB and F. A. GANI, *Mater. Sci. Engng* **72** (1985) 163.
63. P. H. FANG, M. F. KOTKATA and K. M. KANDIL, *J. Non-Cryst. Solids* **89** (1987) 107.
64. R. BECKER, *Ann. Phys.* **32** (1938) 128.
65. U. R. EVANS, *Trans. Faraday Soc.* **41** (1945) 365.
66. J. N. HAY, *Brit. Polym. J.* **3** (1971) 74.

Received 22 March
and accepted 27 November 1991